Biol. Stud., 2025, 19(4), 21–36 • doi: https://doi.org/10.30970/sbi.1904.856
www.https://publications.lnu.edu.ua/journals/index.php/biology

UDC: 576.342+577.352.4+577.12

KINETIC MODELLING OF SULFATE ION TRANSPORT THROUGH BAND 3 PROTEIN OF ERYTHROCYTES

Olga Dotsenko

Vasyl' Stus Donetsk National University, 21 600-richchya St., Vinnytsia 21021, Ukraine

Dotsenko, O. (2025). Kinetic modelling of sulfate ion transport through band 3 protein of erythrocytes. *Studia Biologica*, 19(4), 21–36. doi:10.30970/sbi.1904.856

Background. Assessment of the kinetic properties of ion transport involving band 3 protein (B3p, AE1) is a sensitive tool for monitoring functional changes in erythrocytes under the influence of external factors. The aim of the work was to study the rate of H^+,SO_4^{2-}/Cl exchange in erythrocytes under osmotic and metabolic stress. To achieve this goal, a mathematical model was developed that uses parameter identification methods based on the results of experimental studies.

Materials and Methods. Erythrocytes were incubated in a medium of Na-phosphate buffer (0.015 M, pH 7.4) containing 0.15 M NaCl without glucose. During 3 hours of incubation, the ability of cells to anion exchange, the amount of uptake of SO_4^{2-}, the level of oxidation of sulfhydryl groups and the content of ligand forms of hemoglobin (Hb) in the membrane-bound fraction were tested. To assess anion exchange, a mathematical model was created that involves the search for kinetic parameters using search optimization methods.

Results. The results obtained indicate that under the influence of osmotic and metabolic stress and hypoxia, the work of the anion exchanger AE1 slows down, which is reflected in a decrease in the exchange rate constant HCO_3/Cl, V_{max}, H^+,SO_4^{2-}/Cl exchange. The predicted decrease in the content of SO_4^{2-}-ions in cells is has been confirmed by experimental data. According to the modelling results, incubation of cells leads to activation of the Na^+,K^+,2Cl cotransporter and Na^+/H^+ exchanger, and inhibition of the flux through the K^+,2Cl cotransporter. Assessment of the composition of membrane-bound hemoglobin indicates that the decrease in the speed of AE1 is due to the formation of the deoxyHb-B3p complex and oxidative processes in cells.

Conclusion. The results of mathematical modelling and experimental data indicate the existence of universal O_2-dependent mechanisms of regulation of molecular processes in erythrocytes that are based on competition between deoxyHb and other proteins for binding sites with band 3 protein.

Keywords: sulfate uptake, anion transport, AE1, chloride-bicarbonate antiporters, anion exchange, membrane-bound hemoglobin, ligand forms of hemoglobin, hemichrome, ferrylhemoglobin

INTRODUCTION

Band 3 protein (B3p, AE1) is a major transmembrane protein that occupies a quarter of the surface area of the erythrocyte (RBC) (Jennings, 2021; Remigante *et al*., 2022b; Su *et al*., 2024). B3p is responsible for gas exchange, ion balance, osmotic and mechanical properties of erythrocytes (Morabito *et al*., 2016; Sae-Lee *et al*., 2022; Jin *et al*., 2024). In this regard, even minor modifications of its regulatory sites lead to changes in the cell structure and function (Bertocchio *et al*., 2020; Remigante *et al*., 2022a; Barshtein *et al*., 2024). Band 3 protein consists of three domains: a transmembrane domain that spans the membrane and carries out HCO_3/Cl exchange, a short C-terminal and a long N-terminal cytoplasmic domain (Su *et al*., 2024). The C-terminal cytoplasmic domain binds carbonic anhydrase II, and the N-terminal cytoplasmic domain binds glycolytic enzymes, hemoglobin (Hb), and hemichromes.

Exchange Cl for $HCO_3$of AE1-mediated erythrocyte membrane protein is part of the CO_2 transport in the blood (Jennings, 2005). There are other modes of AE1-mediated transport, including anion conductance and H^+/Cl and H^+,SO_4^{2-}/Cl exchange. These fluxes are much slower than the HCO_3/Cl exchange flux; however, these fluxes are of interest as understanding alternative modes of transport could potentially provide insights into the normal catalytic mechanism of AE1 (Morabito *et al*., 2016; Remigante *et al*., 2022a).

Thus, the anion exchange capacity of B3p can be assessed by measuring the uptake of SO_4^{2-}, which is slower and easier to detect compared to bicarbonate or chloride uptake (Jennings, 2005; Morabito *et al*., 2016; Morabito *et al*., 2020; Remigante *et al*., 2022a; Perrone *et al*., 2023). The SO_4^{2-}/Cl exchange is not electrogenic, as the SO_4^{2-} influx is accompanied by H^+ cotransport (Galtieri *et al*., 2002; Jennings, 2021).

It has been shown (Remigante *et al*., 2022b) that depending on the nature of the stress factors, the rate of H^+,SO_4^{2-}/Cl exchange can either decrease or increase. In particular, H_2O_2 induced oxidative stress leads to a decrease in the SO_4^{2-} uptake rate constant (Morabito *et al*., 2016), while under the influence of a high glucose content, anion exchange is accelerated (Morabito *et al*., 2020). In this regard, an assessment of B3p function by measuring SO_4^{2-} uptake is proposed as a tool for monitoring the effects of various factors on erythrocytes (Morabito *et al*., 2016; Morabito *et al*., 2020; Remigante *et al*., 2022a; Remigante *et al*., 2022b; Perrone *et al*., 2023).

In this work, a rapid test for automatic measurement of extracellular pH is used when cells are placed in a sulfate medium that does not contain Clions. The nature of the change in extracellular pH fully reflects the dynamics of the AE1 function, which carries out H^+,SO_4^{2-}/Cl and HCO_3/Cl exchange. This method is described in detail in the works (Ramazanov, 2011; Nipot, 2012), but is not often used, since the obtained dependences are difficult to interpret.

To analyze the functional changes of the erythrocyte band 3 protein under stress conditions, this research combined the method of measuring extracellular pH with the developed mathematical model describing the transport of SO_4^{2-} ions. The mathematical model is a modification of previous metabolic models (Dotsenko & Taradina, 2024). The model is simplified as much as possible and is used for exploratory optimization of model parameters using experimental data.

The aim of the work was to study the rate of H^+,SO_4^{2-}/Cl exchange in erythrocytes under osmotic and metabolic stress. The research protocol allows a) predicting the course of processes, the content of ions in the cell in accordance with the experimental conditions, b) analyzing experimental data more accurately and qualitatively, c) saving time and money by performing fewer experimental studies. The combination of computational approaches with available experimental data creates the potential for a deep understanding of both the molecular mechanisms and the integrative physiology of anion transport with the participation of B3p.

MATERIALS AND METHODS

Mathematical model and modelling methods. The model describes the ion transport fluxes involved in the changes of extracellular pH during 15 min of cell exposure in a sulphate medium. The model represents a system of ordinary differential equations (ODEs). Each ODE represents the sum of all rates of change of a separate cellular component based on exact kinetic equations. When creating the model, parameter identification methods were applied, the purpose of which was to estimate the "best" set of parameter values that minimizes the error between the experimental data and the model response.

The model construction and all numerical calculations were performed using the COPASI 4.42 modelling environment. The model includes two compartments, in which 10 reactions and ion fluxes occur involving 14 metabolites. The processes involved in the model are presented in **Table 1** and **Fig. 1**.

The estimation of the set of model parameter values is posed as a search optimization problem. The Cocreated model allows calculating the composition of the external and internal environment during the movement of ions. The extracellular space was considered as a well-mixed compartment of an infinite size, and the unmixed layers around the cells were not considered.

Model components. Carbon dioxide. The intracellular content of CO_2 is determined by its production and consumption through: a) intra- and extracellular hydration–dehydration reactions; b) CO_2 exchange with the incubation medium; c) its reactions with hemoglobin.

a) CO_2 hydration occurs by the reaction:

$$CO_2 + H_2O \underset{k_v}{\overset{k_u}{\rightleftarrows}} H_2CO_3 \overset{K}{\rightleftarrows} H^+ + HCO_3^-.$$

In the extracellular environment, CO_2 is hydrated non-enzymatically in cells with the participation of the enzyme carbonic anhydrase (CA). The kinetics of the hydration process was described by the equation (Bidani *et al.*, 1978; Geers & Gros, 2000):

$$v = a \cdot \left(k_u \cdot CO_{2out} - \frac{k_v}{K} H^+_{out} \cdot HCO^-_{3out} \right), \quad (1)$$

where a is a parameter that determines the level of activation of the hydration process with the participation of CA; k_u = 0.137 s^{-1}; k_v = 57.5 s^{-1}; K = 0.35 mM; a = 1 for a non-enzymatic process, a = $3.89 \cdot 10^6$ for an intracellular reaction catalyzed by CA (established during the modelling process).

b) CO_2 diffusion was described by a reverse process $CO_2\_in \underset{k_2}{\overset{k_1}{\rightleftarrows}} CO_2\_out$ as in the works (Geers & Gros, 2000, Michenkova *et al.*, 2021). The diffusion rate was described by the equation:

$$v = k_1 \cdot CO_{2in} - k_2 \cdot CO_{2out},$$

where $k_1 = k_2 = 5.471 \cdot 10^{-3}$ s^{-1} (established during the simulation).

Table 1. **Reactions involved in the model (arrow type, → or ⇄, indicates whether the reaction is considered irreversible or reversible in the analysis)**

No	Reactions	Enzymes
	Medium	
1.	$CO_{2out} + H_2O \rightleftarrows HCO^-_{3out} + H^+_{out}$	
	Cell	
	Jacobs–Stewart cycle	
2.	$CO_{2in} + H_2O \rightleftarrows HCO^-_{3in} + H^+_{in}$	Carbonic anhydrase (CA)
3.	$CO_{2in} \rightleftarrows CO_{2out}$	Transport
4.	$HCO^-_{3out} + Cl^-_{in} \rightleftarrows HCO^-_{3in} + Cl^-_{out}$	AE1 transport
	SO_4^{2-},H^+ cotransport	
5.	$H^+_{out} + SO^{2-}_{4out} + Cl^-_{in} \rightleftarrows H^+_{in} + SO^{2-}_{4in} + Cl^-_{out}$	AE1 transport
	Ion's transport	
	Electroneutral transport	
6.	$K^+_{out} + Cl^-_{out} \rightleftarrows K^+_{in} + Cl^-_{in}$	K^+,Cl cotransporter (KCC)
7.	$K^+_{out} + Na^+_{out} + 2Cl^-_{out} \rightleftarrows K^+_{in} + Na^+_{in} + 2Cl^-_{in}$	Na^+,K^+,2Cl cotransporter (NKCC1)
8.	$Na^+_{out} + H^+_{in} \rightleftarrows Na^+_{in} + H^+_{out}$	Na^+/H^+ exchanger (NE1)
	Hb-buffer's capacity	
9.	$Hb + H^+ \rightleftarrows HHb$	
10.	$Hb + CO_2 \rightleftarrows carbHb + H^+$	

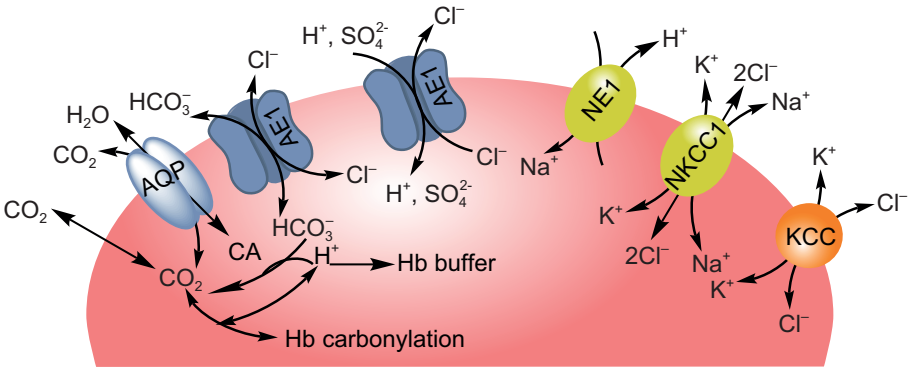

Fig. 1. Scheme of ion transport pathways of the human erythrocyte used in the model. Gradient-driven transport pathways include AE1 (the anion exchange protein 1, B3p), NKCC1 (Na^+,K^+,2Cl cotransporter 1); KCC (K^+,Cl cotransporters), NHE1 (the sodium/hydrogen exchanger), AQP1 (membrane channels are the aquaporins, CA (carbonic anhydrase). Adapted from O. I. Dotsenko & G. V. Taradina (2024)

c) The binding of CO_2 to oxy- and deoxyhemoglobin was described as:

$$Hb \cdot NH_3^+ \underset{}{\overset{K_z}{\rightleftarrows}} Hb \cdot NH_2 + H^+, \quad n\,CO_2 + Hb \cdot NH_2 \underset{K_c}{\overset{k}{\rightleftarrows}} Hb \cdot NHCOO^- + H^+.$$

Since hemoglobin was not introduced into the model as a metabolite, the rate of carbonylation/decarbonylation was described by a modified equation:

$$v = k \cdot \left(\frac{2 \cdot CO_{2in}}{4} \cdot (z_0 + z_1 + z_2) \right), \tag{2}$$

where z_0, z_1, z_2 were described as in C. Geers & G. Gros (2000):

$$z_0 = \frac{1}{\left(CO_{2in} + \frac{H_{in}^+}{K_{c,oxy}} + \frac{H_{in}^{+2}}{K_{c,oxy} \cdot K_{z,oxy}} \right)}, \tag{3}$$

$$z_1 = \frac{1}{\left(CO_{2in} + \frac{H_{in}^+}{K_{c,\alpha\_deoxy}} + \frac{H_{in}^{+2}}{K_{c,\alpha\_deoxy} \cdot K_{z,\alpha\_deoxy}} \right)}, \tag{4}$$

$$z_2 = \frac{1}{\left(CO_{2in} + \frac{H_{in}^+}{K_{c,\beta\_deoxy}} + \frac{H_{in}^{+2}}{K_{c,\beta\_deoxy} \cdot K_{z,\beta\_deoxy}} \right)}, \tag{5}$$

where K_z and K_c are the corresponding equilibrium constants, and k is the rate constant of the direct carbonylation reaction. Binding to the α- and β-chains of deoxyhemoglobin in the presence of 2,3-DPG was described with n = 2, pK_z(α) = 7.32, pK_z(β) = 6.35 and pK_c(α) = 5.04, pK_c(β) = 4.39. Binding to the α-chains of oxyhemoglobin was described with n = 2, pK_z = 6.72, and pK_c = 5.58 (Geers & Gros, 2000). The value of the conditional rate constant was $k = 3.61 \cdot 10^4$ s^{-1} (established from the results of modelling). The magnitude of this constant depends on the ratio between oxy- and deoxyHb in the cells.

Bicarbonate ion. The mass balance of the HCO_3 in each compartment is determined by the rate of the hydration/dehydration reaction catalyzed in the appropriate manner and the HCO_3 flux across the cell membrane.

The transport of HCO_3 through the AE1 carrier was described by the reverse process:

$$HCO_{3out}^- + Cl_{in} \underset{k_2}{\overset{k_1}{\rightleftarrows}} HCO_{3in}^- + Cl_{out}.$$

The exchange of HCO_3 to Cl is described in the work in terms of passive diffusion along an electrochemical gradient.

$$v = \left(k_1 \cdot HCO_{3out}^- - \frac{k_2 \cdot \left(1 + 10^{pHin - pKa}\right)}{1 + \frac{10^{pHin - pKa}}{r}} \cdot HCO_{3in}^- \right), \tag{6}$$

where $k_1 = k_2 = 0.5$ s^{-1}; r – Donnan ratio; $r = \frac{HCO_{3in}^-}{HCO_{3out}^-} = 0.69$; p$K_a$ = 6.3; K_a – first-order dissociation constant of carbonic acid.

Ion transport. In the erythrocyte membrane, there are several types of carriers that carry out passive ion transport. These are Na^+,K^+,2Cl, K^+,Cl cotransporters, Na^+/H^+ exchangers.

K^+,Cl, and Na^+,K^+,2Cl cotransport was described as in the works of V. L. Lew (2023):

$$v_{K^+,Cl^+} = k_{K,Cl} \cdot (K_{out}^+ \cdot Cl_{out}^- - K_{in}^+ \cdot Cl_{in}^-), \tag{7}$$

where $k_{K,Cl}$ – transport rate constant; $k_{K,Cl}$ = 25.39 $mM^{-1}\cdot s^{-1}$.

$$v_{K^+,Na^+,2Cl^-} = k_{K,Na,2Cl}\cdot(K^+_{out}\cdot Na^+_{out}\cdot Cl^{-2}_{out} - K^+_{in}\cdot Na^+_{in}\cdot Cl^{-2}_{in}), \quad (8)$$

where $k_{K,Na,2Cl}$ – transport rate constant; k = 28.4 $M^{-3}\cdot s^{-1}$.

The model parameter values were found by search optimization using experimental data of extracellular pH registration obtained for freshly isolated erythrocytes placed in sulphate medium (0.12 M Na_2SO_4). For this purpose, 30 donor blood samples were used.

The rate of transport through the Na^+/H^+exchanger was described by kinetic equations, according to the work (Yamaguchi *et al*., 2017):

$$v_{Na/H} = \frac{V}{\left(1+\frac{K_{dis}}{H^+_{in}}\right)^n}\cdot\frac{N_{out}\cdot H_{in} - N_{in}\cdot H_{out}}{(1+N_{out}+H_{out})\cdot(N_{in}+H_{in})+(1+N_{in}+H_{in})\cdot(N_{out}+H_{out})}, \quad (9)$$

where V = 0.324 M/s; n = 2.5; $N_{out(in)} = \frac{Na^+_{out(in)}}{K_{Na}}$, $H_{out(in)} = \frac{H^+_{out(in)}}{K_H}$, $Na^+_{out(in)}$, $H^+_{out(in)}$ – concentrations Na^+ and H^+, divided by their respective dissociation constants; K_{dis} – dissociation constant for binding of H^+ at the allosteric modification site (K_{dis} = 1.41·10^{-7}); n – Hill coefficient; K_{Na} = 0.012, K_H = 4.467·10^{-9}. The value K_{Na},K_H was found through search optimization using experimental data.

H^+,SO_4^{2-} transport. H^+,SO_4^{2-} transport was described by Michaelis–Menten kinetics for a bisubstrate process. The absence of SO_4^{2-} in the erythrocyte ensures that the intracellular SO_4^{2-} content is essentially an indicator of anion uptake (Galtieri *et al*., 2002):

$$v = \frac{V_{max}\cdot H\cdot SO^{2-}_{4out}}{\left(K_{mH^+}+H^+_{out}\right)\cdot\left(K_{mSO_4^{2-}}+SO^{2-}_{4out}\right)}, \quad (10)$$

where V_{max} – maximum H^+,SO_4^{2-}/Cl transport rate (V_{max} = 14.6 mM/s); K_{mH^+}, $K_{mSO_4^{2-}}$ – Michaelis constant; K_{mH^+} = 1.46 mM; $K_{mSO_4^{2-}}$ = 4.16 mM.

Hydrogen ions. H^+ changes in cells occur due to hydration-dehydration of CO_2, the action of the hemoglobin buffer, carbamate formation, oxygenation-deoxygenation of hemoglobin, and with the participation of the transport processes described above.

Buffer cellular reactions. Buffering of protons by hemoglobin occurs according to the reactions:

$$bH^+ + Hb\cdot NH_2 \underset{K_c}{\overset{k_a}{\rightleftarrows}} Hb\cdot NH_3^+,$$

$$bH^+ + HbO_2\cdot NH_2 \underset{K_c}{\overset{k_a}{\rightleftarrows}} HbO_2\cdot NH_3^+.$$

The rate of the process was described:

$$v = k_a\cdot(H^+_{in})^b - K_c, \quad (11)$$

where k_a = 7.5·10^3 s^{-1}, apparent protonation constant; K_c – apparent dissociation constant (K_c = 3.17·10^{-5}, b = 1). The values of these parameters depend on the ratio between oxy- and deoxyHb in the cells.

Estimation of model parameters. Parameter estimation enables the identification of a parameter vector that minimizes the discrepancy between model predictions and experimental data. This approach integrates mathematical modelling with experimental studies, providing a more reliable understanding of the processes under investigation, as well as allowing the estimation of unknown model parameters or the assessment of their temporal dynamics.

Parameter estimation was performed using experimental data presented as time dependences of extracellular pH from 900 points. When studying the influence of incubation conditions on the functionality of AE1, the objective function was minimized using 12 model parameters ($CO_2(0)\_in$, $HCO_3^-(0)\_in$, $k_{HCO_3^-/Cl^-}$, $k_{K,Cl}$, $k_{K,Na,2Cl}$, $V_{Na/H}$, K_{Na^+}, $V_{max H^+,SO_4^{2-}}$, K_{mH^+}, $K_{mSO_4^{2-}}$, k_a, K_c).

The objective function has the form:

$$O(p) = \sum_j \sum_k \left(pH_{k,j} - pH_{k,j}(p)\right)^2,$$

where $pH_{k,j}$ the experimental value of extracellular pH at measurement j in experiment k and the corresponding calculated value $pH_{k,j}(p)$, where p is the vector of estimated parameters during modelling.

In the work, the search for parameters was performed using the evolutionary programming method, which is implemented in COPASI. The result of the search optimization is a set of kinetic parameters of the model.

When solving the system of equations with the parameters found during the search optimization, the kinetic dependences of ion concentrations and fluxes of the corresponding processes of the model were obtained.

Experimental studies. Erythrocytes were obtained from the capillary blood of healthy female donors of approximately the same age (45±5.5 years). All participants provided written informed consent. The Declaration of Helsinki (2000) and relevant national standards for volunteer participation in research were taken into account. The erythrocytes were separated from the plasma by centrifugation, washed with Na-phosphate buffer (0.015 M, pH 7.4) (buffer solution 1) containing 0.15 M NaCl. The leukocyte film and supernatant were removed by aspiration.

The erythrocytes were transferred to the medium of the same buffer solution 1 without glucose and incubated for 3 hours at 20 °C. The hemoglobin content in the studied suspensions was at the level of 3±0.18 mg/mL. Throughout the experiment, the studied system was in contact with ambient air.

Study of H^+ transport in sulfate medium. Every 30 min, 2 mL of suspension was taken from the experimental sample, the liquid was removed by centrifugation (2 min, 3000 rpm). After addition of Na_2SO_4 (2 mL, 0.12 M) to the obtained cell precipitate, extracellular pH changes were recorded for 15 min with a step of 1 s (Ramazanov, 2011; Nipot, 2012). A glass combined electrode ESC-10612 was used to record pH. The pH change was recorded in automatic mode. The experiment was performed at a temperature of 20 °C in five replicates. The obtained experimental dependences were used for mathematical modelling.

Sulfate transport measurement. This study was conducted to assess the reliability of the results of mathematical modelling.

Every 20 min, 2 mL of the suspension was taken, from which the cells were precipitated by centrifugation. Cells were incubated in Na_2SO_4 solution (2 mL, 0.12 M) for 15 min. The incubation medium was removed by centrifugation, the cells were washed from sulfate ions with buffer solution 1. Erythrocytes were lysed with 2 mL H_2O, after which the proteins were precipitated by adding 0.5 mL of 55% trichloroacetic acid (TCA) and separated by centrifugation. To 1 mL of the supernatant was added 1 mL of a mixture of glycerol-water (1:1), 0.5 mL of 4M NaCl and 1M HCl, 0.5 mL of 1.23 M $BaCl_2$. The absorbance of this suspension was measured at 360 nm. A standard calibration

curve was used to quantify the sulfate ion content (Galtieri *et al*., 2002; Tellone *et al*., 2008; Perrone *et al*., 2023).

Study of the content of ligand forms of hemoglobin in the membrane-bound fraction. The quantitative assessment of ligand-bound forms of membrane-associated hemoglobin was performed using erythrocyte ghosts, based on absorption spectra. The procedure is described in detail in (Attia *et al*., 2015; Ratanasopa *et al*., 2015; Meng & Alayash, 2017). The content of each form was expressed as a percentage of the total hemoglobin content in the membrane-bound fraction.

Study of the content of SH groups. Erythrocytes taken from the incubation medium were lysed in 0.5 mL of cold water, after which 2.5 mL of the precipitation mixture (19.6 mL of 85% H_3PO_4, 2 g EDTA, 50 g NaCl per 500 mL of water) was added. After 20 min, the precipitate was separated by centrifugation. The precipitate was dissolved in 0.3 M Na_2HPO_4, pH 8.8, containing 5% DDS at 37 °C. The content of SH groups was determined using Ellman's reagent. The content of SH groups of erythrocyte proteins in μM per g of hemoglobin (Hb) in the sample was determined using the calibration curve constructed for GSH.

The results were analyzed using Statistica 8.0 (StatSoft Inc., USA). Experimental data are presented as x ± SE (x is the mean, SE is the relative error).

RESULTS

Fig. 2 presents the experimental dependences of the pH change of the erythrocyte suspension in a sulphate medium (0.12 M Na_2SO_4), which does not contain buffer components and Cl ions. In this case, a two-phase change in the pH of the external environment occurs.

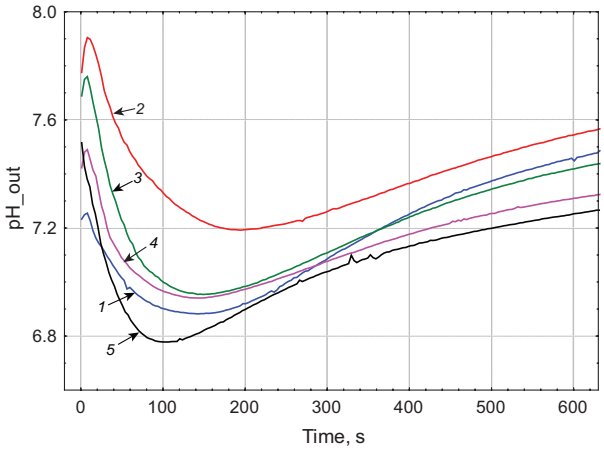

Fig. 2. Experimental dependences of the pH change of a 0.12 M Na_2SO_4 after its addition to the erythrocyte pellet. Incubation time of cells in buffer solution 1: *1* – 0; *2* – 30; *3* – 60; *4* – 120; *5* – 180 min

The simulation results are presented in **Figs 3**, **4** and in **Table 2**.

The experimental dependence of the accumulation of SO_4^{2-} ions in erythrocytes after their movement from the incubation medium into the Na_2SO_4 solution is shown in **Fig. 5*A***. The incubation time of erythrocytes in the sulfate medium coincided with the time of H^+ transport measurement. It can be seen that incubation of cells in a buffer solution without glucose significantly reduces the ability of cells to accumulate sulphate (before incubation, the SO_4^{2-} content was 917.5 ± 117.7 mM, after three hours of incubation – 674.7±53.7 mM. The obtained experimental data coincide with the modelling results (**Fig. 4*B***).

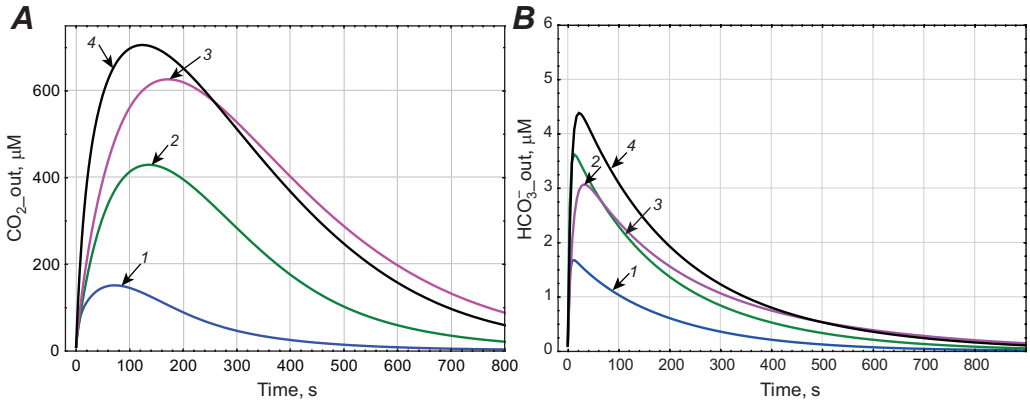

Fig. 3. Changes in the content of CO_2 (***A***) and HCO_3 (***B***) in the extracellular medium containing sulfate. Dependencies obtained during mathematical modelling. Incubation time of cells in buffer solution 1: *1* – 0; *2* – 60; *3* – 120; *4* – 180 min

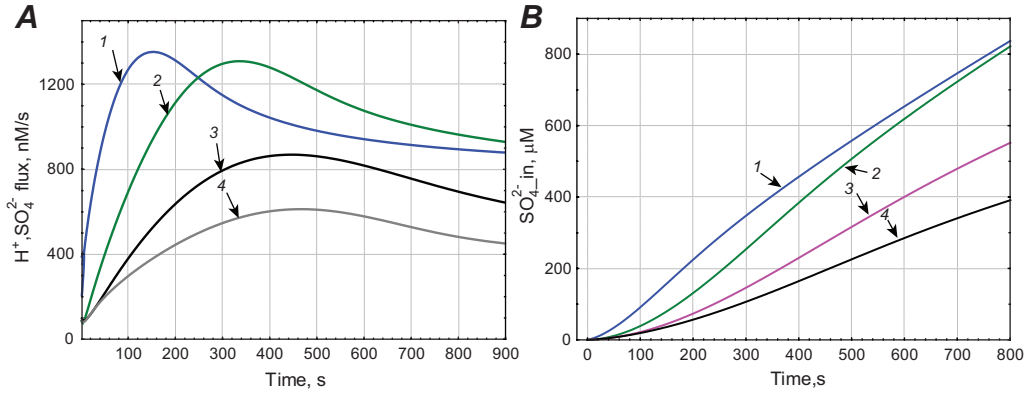

Fig. 4. The H^+,SO_4^{2-} flux through Bp3 (***A***) and change in cell SO_4^{2-} content (***B***) after their movement from the incubation medium into the sulfate medium. Dependencies obtained during mathematical modelling. Incubation time of cells in buffer solution 1: *1* – 0; *2* – 60; *3* – 120; *4* – 180 min

Table 2. **Optimized parameters of the mathematical model**

Time, min	V_{max}, mM/s H^+,SO_4^{2-} cotransport	k_{H^+/HCO_3^-} exchange, s^{-1}	V_{Na^+/H^+}, mM/s	$k_{K^+/Na^+/2Cl^-}$ cotransport, $M^{-3}\cdot s^{-1}$	k_{K^+/Cl^-} cotransport, $mM^{-2}\cdot s^{-1}$
0	14.65±5.54	0.49±0.12	55.46±5.18	28.4±5.18	25.39±6.15
30	10.91±2.05	*0.21±0.17	51.77±6.16	5.09±1.16	18.60±2.82
60	10.56±2.63	*0.19±0.15	*148.9±12.8	21.2±2.8	*13.05±5.75
90	*3.51±1.64	*0.21±0.13	*141.6±9.01	*43.4±9.01	*10.08±3.49
120	*2.56±1.23	*0.06±0.013	*233.4±14.5	*251.1±14.5	*10.50±6.07
150	*4.23±1.49	*0.06±0.065	*488.2±20.1	*228.2±20.1	*11.82±2.46
180	*2.49±0.81	*0.09±0.03	*509.9±19.1	*218.9±19.1	*11.04±3.92

Note: *– changes are significant compared to the initial state

The content of SH groups in erythrocyte proteins during 120 min of the experiment did not significantly change (**Fig. 5*B***). During the last hour of incubation, the content of SH groups decreased by 1.7±0.3 times relative to the initial level.

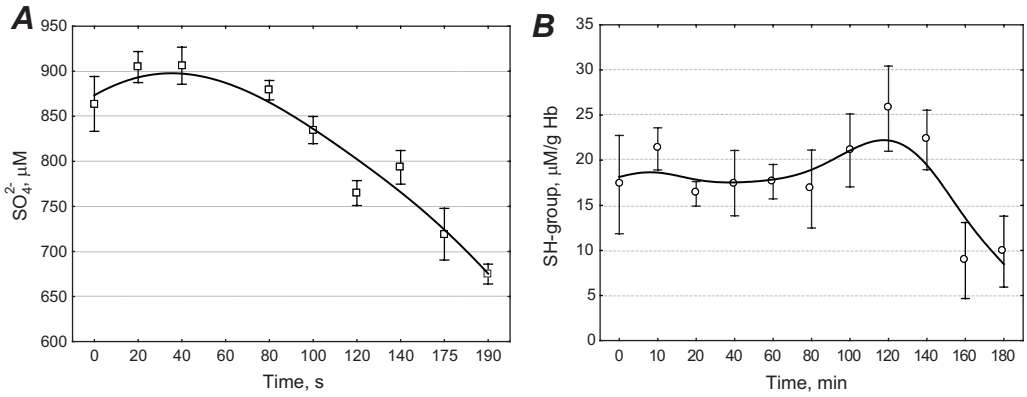

Fig. 5. Accumulation of SO_4^{2-} ions in cells (***A***), content of SH groups in proteins of erythrocytes (***B***) incubated in buffer solution 1. Each point is represented as x ± SE for n = 5

In the membrane-bound fraction, after 60–90 min of incubation, a decrease in oxyhemoglobin (oxyHb) to 58.3±2.6% was recorded; the content of deoxyhemoglobin (deoxyHb) was 12.1±3.4%, and methemoglobin (metHb) was 30.6±3.18%. At the end of the experiment, the content of metHb increased to 37.42±1.18%. In the membrane-bound fraction, the presence of hemichromes and ferrylhemoglobin (FerrylHb) (up to 0.37±0.11%) was recorded (**Fig. 6**).

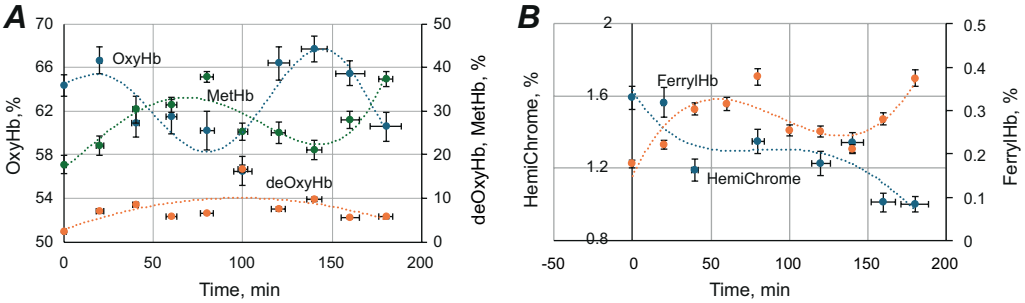

Fig. 6. Distribution of ligand forms of hemoglobin in the membrane-bound fraction of erythrocytes incubated in buffer solution 1. Each point is represented as x ± SE for n = 5

DISCUSSION

Incubation of erythrocytes in a glucose-free medium results in metabolic disturbances and a rapid depletion of ATP. The effect of saline solution (buffer solution 1) on erythrocytes was investigated by O. I. Dotsenko & G. V. Taradina (2024). It was found that under these incubation conditions, cells lose K^+ and Cl^- ions and increase the content of Na^+ ions, which results in a decrease in cell volume.

The same incubation medium was used to study the work of Bp3. According to the simulation results (**Fig. 3**), the addition of Na_2SO_4 to the erythrocyte suspension is accompanied by the release of carbon dioxide into the extracellular environment with subsequent hydration with the formation of HCO_3 and H^+. The simulation results indicate that the flux of sulphate is not delayed in time; therefore, the entry of H^+ into the cells stimulates the outflux of CO_2.

Physiologically, B3p provides a balance between internal and external anions, such as Cl and HCO_3, which are distributed according to the transmembrane potential. Anions are transported by a ping-pong mechanism, where only the loaded transport site can pass through the membrane (Gimsa, 1995). As has been shown (Gimsa, 1995), the B3p conformers are asymmetrically distributed, with about 90% of the transport sites facing the inside. Low external concentrations of Cl^- can recruit the B3p transport site to the external solution (Gimsa, 1995). Since under normal conditions, 90% of the transport sites face the cytoplasm, recruitment of the external conformers will involve almost all B3p proteins. This explains the sharp increase in HCO_3 in the extracellular medium during the first seconds after placing the cells in Na_2SO_4 solution (**Fig. 3*B***), which results in the creation of a driving force for net influx HCO_3 in exchange for Cl (Jennings, 2013). Reduced CO_2_out creates a driving force for diffusive efflux of CO_2.

Next, there is mainly an exchange of HCO_3, H^+,SO_4^{2-} in exchange for intracellular Cl. The extracellular pH decreases (**Fig. 2**), because the rate of hydration exceeds the rate of H^+,SO_4^{2-} cotransport.

Model calculations show that the flux of SO_4^{2-} ions into the cell is biphasic (**Fig. 4*A***). The flux of CO_2 from the cell allows increasing the amount of H^+ in the extracellular medium, which stimulates the flux of sulphate (**Fig. 4*A***). The observed elevation of extracellular H^+ levels can be partially explained by the contribution of the Na^+/H^+ exchanger, whose activity rises by nearly an order of magnitude toward the end of incubation (**Table 2**).

The intracellular and extracellular activities of HCO_3 are linked to the corresponding activities of H^+ through hydration/dehydration reactions between HCO_3 and carbon dioxide. This reaction is catalyzed by the enzyme carbonic anhydrase in the intracellular compartment (Al-Samir *et al*., 2013) and proceeds at an uncatalyzed rate in the extracellular compartment, making the extracellular reactions rate-limiting for acid balance relative to the erythrocyte membrane (Nikinmaa, 2003).

As equilibrium $CO_2 + H_2O \underset{k_v}{\overset{k_u}{\rightleftarrows}} H_2CO_3 \overset{K}{\rightleftarrows} H^+ + HCO_3^-$ in the extracellular environment approaches, the condition of which is $[CO_2] = \frac{k_v \cdot [H^+] \cdot [HCO_3^-]}{K \cdot k_u}$, the H^+ content decreases. Thus, it becomes clear that the increase in pH in the extracellular environment is not due to an increase in the flow of SO_4^{2-} into the cell (Nipot, 2012), but to a decrease in the flows of HCO_3 and CO_2 as a result of approaching equilibrium.

The changes that occurred in the cells during incubation in a buffer solution are reflected by the values of the model parameters found during the search optimization. The search optimization of the model parameters shows a decrease in the rate constant of the HCO_3/H^+ exchange, V_{max} H^+,SO_4^{2-}/Cl^- exchange in erythrocytes with the incubation time (**Table 2**). At the same time, K_{mH^+} and $K_{mSO_4^{2-}}$ did not change significantly. The modelling results show that an increase in the cell incubation time in a buffer solution without glucose leads to a decrease in the rate of anion exchange B3p, which results in a decrease in the content of SO_4^{2-}-ions in the cells. The modelling results are confirmed by experimental data on the uptake of SO_4^{2-}-ions (**Fig. 5*A***).

The most likely candidate for the role of a switch for metabolism and ion transport in mammalian erythrocytes during hypoxia is membrane-bound hemoglobin (Welbourn *et al*., 2017). Binding of deoxyHb to cdAE1 is likely to reduce the activity of the erythrocyte anion exchanger (Cilek *et al*., 2024), although direct evidence is not yet available. It has been suggested that binding of deoxyHb to AE1 may inhibit AE1 clustering induced by oxidized forms of hemoglobin.

According to the simulation results, the rate constant of HCO_3/Cl exchange after 30 min of incubation under experimental conditions decreases by two times, and after 120 min – by 5–8 times. Along with this, we recorded a significant decrease in -SH groups in the protein fraction (**Fig. 5*A***) and an increase in the content of metHb and FerrylHb in membrane-bound hemoglobin (**Fig. 6**). As was shown (Yang *et al*., 2024), the formation of disulfide bonds weakens dephosphorylation and promotes phosphorylation of a number of acidic amino acids of B3p by Syk and Lyn tyrosine kinases (Cilek *et al*., 2024). As a result, the binding of B3p to anchor proteins decreases (Ferru *et al*., 2011), and the mobility increases, which leads to B3p aggregation.

Partial oxygenation of hemoglobin dramatically increases the rate of hemoglobin autoxidation (Yang *et al*., 2024), with the formation of oxidized forms of hemoglobin, hemichromes, and ferrylhemoglobin (FerrylHb). These forms of hemoglobin have a much higher affinity for the erythrocyte membrane, creating irreversible cross-linking involving both B3p and spectrin (Ferru *et al*., 2011). This binding disrupts the interaction between B3p and cytoskeletal proteins (ankyrin and spectrin) and triggers B3p clustering (Welbourn *et al*., 2017; Cilek *et al*., 2024; Barshtein *et al*., 2024; Yang *et al*., 2024).

According to the simulation results, incubation of cells leads to activation of the Na^+,K^+,2Clcotransporter and the Na^+/H^+ exchanger, and inhibition of the flux through the K^+,Cl cotransporter (**Table 2**). Na^+,K^+,2Cl, K^+,Cl cotransporters and Na^+/H^+ exchanger are known to be O_2-dependent (Zheng *et al*., 2019). In human erythrocytes, this cotransport is largely inactive in oxygenated cells but is activated in deoxygenated erythrocytes (Zheng *et al*., 2019; Cilek *et al*., 2024).

It has been experimentally demonstrated (Zheng *et al*., 2019) that deoxyHb binds to the cytoplasmic domain of B3p and displaces the WNK1 kinase from its docking site on B3p. The displaced WNK1 kinase activates OSR1, which in turn phosphorylates and activates the Na^+,K^+,2Cl cotransporter.

Since the effect of O_2 on K^+,Cl cotransport is opposite to its effect on Na^+,K^+,2Cl cotransport, and the phosphorylation sites on these cotransporters are homologous, Zheng *et al*. (2019) proposed that the displacement of WNK1 by deoxyHb may underlie the inhibition or activation of these cotransport pathways.

In most cases studied, the activity of Na^+/H^+exchange increases with deoxygenation, regardless of the underlying stimulus causing the increase in fluxes (Nikinmaa, 2003).

According to the results of mathematical modelling, incubation of erythrocytes under the studied conditions leads to an increase in the activity of the Na^+/H^+ exchanger, especially after the 2nd hour of incubation. After placing these cells in a sulfate medium, a sharp decrease in extracellular pH is observed (**Fig. 2**), which is due to the flow through this carrier.

Na^+/H^+ exchange causes a net influx of Na^+ and efflux of H^+, displacing H^+ from electrochemical equilibrium during the initial minutes of activation. Net excretion of protons occurs as long as the rate Na^+/H^+ exchange is higher than the rate-limiting step of passive proton equilibrium, extracellular HCO_3 dehydration, and protons to carbon dioxide (Nikinmaa, 2003; Barshtein *et al*., 2024).

CONCLUSION

The created mathematical model allows us to understand not only the molecular mechanism of H^+,SO_4^{2-}/Cl exchange, but also to investigate changes in ion transport in erythrocytes under external influences. Data on the changes in pH of the erythrocyte suspension in a sulfate medium, which does not contain buffering components and Cl ions, are used for the optimization of the model parameters.

The applied approach allowed us to establish that in erythrocytes, under the influence of osmotic and metabolic stress and hypoxia, the work of the anion exchanger AE1 slows down, which is reflected in a decrease in the rate constants of the HCO_3/Cl exchange, V_{max} H^+,SO_4^{2-}/Cl exchange.

The model predicts a decrease in the content of SO_4^{2-} ions in cells, which is confirmed by experimental data. According to the simulation results, incubation of cells leads to the activation of the Na^+,K^+,2Cl cotransporter and the Na^+/H^+ exchanger, and inhibition of the flux through the K^+,Cl^- cotransporter. Experimental studies of the composition of membrane-bound hemoglobin show that the deoxyHb-B3p complex is a trigger for processes that adapt erythrocytes to changed conditions, in particular hypoxia.

COMPLIANCE WITH ETHICAL STANDARDS

Human Rights: all studies were conducted following the guidelines outlined in the Declaration of Helsinki. Approval for the study was obtained from the ethics committee of Vasyl' Stus Donetsk National University (protocol No 1 of January 11, 2025).

REFERENCES

Al-Samir, S., Papadopoulos, S., Scheibe, R. J., Meißner, J. D., Cartron, J., Sly, W. S., Alper, S. L., Gros, G., & Endeward, V. (2013). Activity and distribution of intracellular carbonic anhydrase II and their effects on the transport activity of anion exchanger AE1/SLC4A1. *The Journal of Physiology*, 591(20), 4963–4982. doi:10.1113/jphysiol.2013.251181
Crossref ● PubMed ● PMC ● Google Scholar

Attia, A. M. M., Ibrahim, F. A. A, Abd El-Latif, N. A., Aziz, S. W., & Moussa, S. A. A. (2015). Biophysical study on conformational stability against autoxidation of oxyhemoglobin and erythrocytes oxidative status in humans and rats. *Wulfenia Journal*, 22(12), 264–281.
Google Scholar

Barshtein, G., Livshits, L., Gural, A., Arbell, D., Barkan, R., Pajic-Lijakovic, I., & Yedgar, S. (2024). Hemoglobin binding to the red blood cell (RBC) membrane is associated with decreased cell deformability. *International Journal of Molecular Sciences*, 25(11), 5814. doi:10.3390/ijms25115814
Crossref ● PubMed ● PMC ● Google Scholar

Bidani, A., Crandall, E. D., & Forster, R. E. (1978). Analysis of postcapillary pH changes in blood *in vivo* after gas exchange. *Journal of Applied Physiology*, 44(5), 770–781. doi:10.1152/jappl.1978.44.5.770
Crossref ● PubMed ● Google Scholar

Bertocchio, J. P., Genetet, S., Da Costa, L., Walsh, S. B., Knebelmann, B., Galimand, J., Bessenay, L., Guitton, C., De Lafaille, R., Vargas-Poussou, R., Eladari, D., & Mouro-Chanteloup, I. (2020). Red blood cell AE1/band 3 transports in dominant distal renal tubular acidosis patients. *Kidney International Reports*, 5(3), 348–357. doi:10.1016/j.ekir.2019.12.020
Crossref ● PubMed ● PMC ● Google Scholar

Bruce, L. J., Beckmann, R., Ribeiro, M. L., Peters, L. L., Chasis, J. A., Delaunay, J., Mohandas, N., Anstee, D. J., & Tanner, M. J. (2003). A band 3-based macrocomplex of integral and peripheral proteins in the RBC membrane. *Blood*, 101(10), 4180–4188. doi:10.1182/blood-2002-09-2824
Crossref ● PubMed ● Google Scholar

Cilek, N., Ugurel, E., Goksel, E., & Yalcin, O. (2023). Signaling mechanisms in red blood cells: a view through the protein phosphorylation and deformability. *Journal of Cellular Physiology*, 239(3), e30958. doi:10.1002/jcp.30958
Crossref ● PubMed ● Google Scholar

Dotsenko, O. I., & Taradina, G. V. (2024). Ion homeostasis in the regulation of intracellular pH and volume of human erythrocytes. *Biophysical Bulletin*, 51, 7–25. doi:10.26565/2075-3810-2024-51-01
Crossref ● Google Scholar

Ferru, E., Giger, K., Pantaleo, A., Campanella, E., Grey, J., Ritchie, K., Vono, R., Turrini, F., & Low, P. S. (2011). Regulation of membrane-cytoskeletal interactions by tyrosine phosphorylation of erythrocyte band 3. *Blood*, 117(22), 5998–6006. doi:10.1182/blood-2010-11-317024
Crossref ● PubMed ● PMC ● Google Scholar

Galtieri, A., Tellone, E., Romano, L., Misiti, F., Bellocco, E., Ficarra, S., Russo, A., Di Rosa, D., Castagnola, M., Giardina, B., & Messana, I. (2002). Band-3 protein function in human erythrocytes: effect of oxygenation–deoxygenation. *Biochimica et Biophysica Acta* (*BBA*) – *Biomembranes*, 1564(1), 214–218. doi:10.1016/s0005-2736(02)00454-6
Crossref ● PubMed ● Google Scholar

Geers, C., & Gros, G. (2000). Carbon dioxide transport and carbonic anhydrase in blood and muscle. *Physiological Reviews*, 80(2), 681–715. doi:10.1152/physrev.2000.80.2.681
Crossref ● PubMed ● Google Scholar

Gimsa, J. (1995). Red cell echinocytogenesis is correlated to the recruitment of external band-3 conformations. *Bioelectrochemistry and Bioenergetics*, 38(1), 99–103. doi:10.1016/0302-4598(95)01794-f
Crossref ● Google Scholar

Jennings, M. L. (2005). Evidence for a second binding/transport site for chloride in erythrocyte anion transporter AE1 modified at glutamate 681. *Biophysical Journal*, 88(4), 2681–2691. doi:10.1529/biophysj.104.056812
Crossref ● PubMed ● PMC ● Google Scholar

Jennings, M. L. (2013). Transport of H_2S and HS^- across the human red blood cell membrane: rapid H_2S diffusion and AE1-mediated Cl^-/HS^- exchange. *American Journal of Physiology. Cell Physiology*, 305(9), C941–C950. doi:10.1152/ajpcell.00178.2013
Crossref ● PubMed ● PMC ● Google Scholar

Jennings, M. L. (2021). Cell physiology and molecular mechanism of anion transport by erythrocyte band 3/AE1. *American Journal of Physiology. Cell Physiology*, 321(6), C1028–C1059. doi:10.1152/ajpcell.00275.2021
Crossref ● PubMed ● PMC ● Google Scholar

Jin, X., Zhang, Y., Wang, D., Zhang, X., Li, Y., Wang, D., Liang, Y., Wang, J., Zheng, L., Song, H., Zhu, X., Liang, J., Ma, J., Gao, J., Tong, J., & Shi, L. (2024). Metabolite and protein shifts in mature erythrocyte under hypoxia. *iScience*, 27(4), 109315. doi:10.1016/j.isci.2024.109315
Crossref ● PubMed ● PMC ● Google Scholar

Lew, V. L. (2023). The circulatory dynamics of human red blood cell homeostasis: oxy-deoxy and PIEZO1-triggered changes. *Biophysical Journal*, 122(3), 484–495. doi:10.1016/j.bpj.2022.12.038
Crossref ● PubMed ● PMC ● Google Scholar

Meng, F., & Alayash, A. I. (2017). Determination of extinction coefficients of human hemoglobin in various redox states. *Analytical Biochemistry*, 521, 11–19. doi:10.1016/j.ab.2017.01.002
Crossref ● PubMed ● PMC ● Google Scholar

Michenkova, M., Taki, S., Blosser, M. C., Hwang, H. J., Kowatz, T., Moss, Fraser. J., Occhipinti, R., Qin, X., Sen, S., Shinn, E., Wang, D., Zeise, B. S., Zhao, P., Malmstadt, N., Vahedi-Faridi, A., Tajkhorshid, E., & Boron, W. F. (2021). Carbon dioxide transport across membranes. *Interface Focus*, 11(2), 20200090. doi:10.1098/rsfs.2020.0090
Crossref ● PubMed ● PMC ● Google Scholar

Morabito, R., Romano, O., La Spada, G., & Marino, A. (2016). H_2O_2-induced oxidative stress affects $SO_4^=$ transport in human erythrocytes. *PloS One*, 11(1), e0146485. doi:10.1371/journal.pone.0146485
Crossref ● PubMed ● PMC ● Google Scholar

Morabito, R., Remigante, A., Spinelli, S., Vitale, G., Trichilo, V., Loddo, S., & Marino, A. (2020). High glucose concentrations affect band 3 protein in human erythrocytes. *Antioxidants*, 9(5), 365. doi:10.3390/antiox9050365
Crossref ● PubMed ● PMC ● Google Scholar

Nikinmaa, M. (2003). Gas transport. In: I. Bernhardt, J. C. Ellory (Eds), *Red cell membrane transport in health and disease* (pp. 489–509). Berlin: Springer, Berlin, Heidelberg. doi:10.1007/978-3-662-05181-8_20
Crossref ● Google Scholar

Nipot, E. (2012). Effect of butanol and hexanol on the anion transport in ram and hen red blood cells. *Visnyk of the Lviv University. Series Biology*, 58, 246–250. (In Ukrainian)
Google Scholar

Perrone, P., Spinelli, S., Mantegna, G., Notariale, R., Straface, E., Caruso, D., Falliti, G., Marino, A., Manna, C., Remigante, A., & Morabito, R. (2023). Mercury chloride affects band 3 protein-mediated anionic transport in red blood cells: role of oxidative stress and protective effect of olive oil polyphenols. *Cells*, 12(3), 424. doi:10.3390/cells12030424
Crossref ● PubMed ● PMC ● Google Scholar

Ramazanov, V. V. (2011). Efficiency of combined cryopreservatives containing glycerol or 1,2-propanediol during freezing of erythrocytes. *Problems of Cryobiology and Cryomedicine*, 21(2), 125–136. Retrieved from https://journal.cryo.org.ua/index.php/probl-cryobiol-cryomed/article/view/138
Google Scholar

Ratanasopa, K., Strader, M. B., Alayash, A. I., & Bulow, L. (2015). Dissection of the radical reactions linked to fetal hemoglobin reveals enhanced pseudoperoxidase activity. *Frontiers in Physiology*, 6, 39. doi:10.3389/fphys.2015.00039
Crossref ● PubMed ● PMC ● Google Scholar

Remigante, A., Spinelli, S., Trichilo, V., Loddo, S., Sarikas, A., Pusch, M., Dossena, S., Marino, A., & Morabito, R. (2022a). d-Galactose induced early aging in human erythrocytes: role of band 3 protein. *Journal of Cellular Physiology*, 237(2), 1586–1596. doi:10.1002/jcp.30632
Crossref ● PubMed ● PMC ● Google Scholar

Remigante, A., Spinelli, S., Pusch, M., Sarikas, A., Morabito, R., Marino, A., & Dossena, S. (2022b). Role of SLC4 and SLC26 solute carriers during oxidative stress. *Acta Physiologica*, 235(1), e13796. doi:10.1111/apha.13796
Crossref ● PubMed ● PMC ● Google Scholar

Sae-Lee, W., McCafferty, C. L., Verbeke, E. J., Havugimana, P. C., Papoulas, O., McWhite, C. D., Houser, J. R., Vanuytsel, K., Murphy, G. J., Drew, K., Emili, A., Taylor, D. W., & Marcotte, E. M. (2022). The protein organization of a red blood cell. *Cell Reports*, 40(3), 111103. doi:10.1016/j.celrep.2022.111103
Crossref ● PubMed ● PMC ● Google Scholar

Su, C. C., Zhang, Z., Lyu, M., Cui, M., & Yu, E. W. (2024). Cryo-EM structures of the human band 3 transporter indicate a transport mechanism involving the coupled movement of chloride and bicarbonate ions. *PLoS Biology*, 22(8), e3002719. doi:10.1371/journal.pbio.3002719
Crossref ● PubMed ● PMC ● Google Scholar

Tellone, E., Ficarra, S., Scatena, R., Giardina, B., Kotyk, A., Russo, A., Colucci, D., Bellocco, E., Laganà, G., & Galtieri, A. (2008). Influence of gemfibrozil on sulfate transport in human erythrocytes during the oxygenation-deoxygenation cycle. *Physiological Research*, 57(4), 621–629. doi:10.33549/physiolres.931251
Crossref ● PubMed ● Google Scholar

Welbourn, E. M., Wilson, M. T., Yusof, A., Metodiev, M. V., & Cooper, C. E. (2017). The mechanism of formation, structure and physiological relevance of covalent hemoglobin attachment to the erythrocyte membrane. *Free Radical Biology & Medicine*, 103, 95–106. doi:10.1016/j.freeradbiomed.2016.12.024
Crossref ● PubMed ● PMC ● Google Scholar

Yamaguchi, M., Steward, M. C., Smallbone, K., Sohma, Y., Yamamoto, A., Ko, S. B., Kondo, T., & Ishiguro, H. (2017). Bicarbonate-rich fluid secretion predicted by a computational model of guinea-pig pancreatic duct epithelium. *The Journal of Physiology*, 595(6), 1947–1972. doi:10.1113/jp273306
Crossref ● PubMed ● PMC ● Google Scholar

Yang, Q., Chen, D., Li, C., Liu, R., & Wang, X. (2024). Mechanism of hypoxia-induced damage to the mechanical property in human erythrocytes-band 3 phosphorylation and sulfhydryl oxidation of membrane proteins. *Frontiers in Physiology*, 15, 1399154. doi:10.3389/fphys.2024.1399154
Crossref ● PubMed ● PMC ● Google Scholar

Zheng, S., Krump, N. A., McKenna, M. M., Li, Y. H., Hannemann, A., Garrett, L. J., Gibson, J. S., Bodine, D. M., & Low, P. S. (2019). Regulation of erythrocyte $Na^+/K^+/2Cl^-$ cotransport by an oxygen-switched kinase cascade. *The Journal of Biological Chemistry*, 294(7), 2519–2528. doi:10.1074/jbc.ra118.006393
Crossref ● PubMed ● PMC ● Google Scholar

КІНЕТИЧНЕ МОДЕЛЮВАННЯ ТРАНСПОРТУ СУЛЬФАТ-ІОНІВ КРІЗЬ БІЛОК СМУГИ 3 ЕРИТРОЦИТІВ

Ольга Доценко

Донецький національний університет імені Василя Стуса
вул. 600-річчя, 21, Вінниця 21021, Україна

Обґрунтування. Оцінка кінетичних властивостей іонного транспорту за участю білка смуги 3 (B3p, AE1) є чутливим інструментом для моніторингу функціональних змін еритроцитів під дією зовнішніх чинників. Мета роботи полягала в дослідженні швидкості аніонного обміну $H^+,SO_4^{2-}/Cl$ в еритроцитах, що перебували в умовах осмотичного і метаболічного стресу. Для досягнення поставленої мети розроблено математичну модель, що використовує методи ідентифікації параметрів на основі результатів експериментальних досліджень.

Матеріали та методи. Еритроцити інкубували у середовищі Na-фосфатному буфері (0,015 М, pH 7.4), що містив 0,15 М NaCl без глюкози. Упродовж 3-х год інкубування тестували здатність клітин до аніонного обміну, кількість поглинутого SO_4^{2-}, рівень окислення сульфгідрильних груп і вміст лігандних форм гемоглобіну у складі мембранозв'язаної фракції. Для оцінки аніонного обміну створено математичну модель, яка передбачає пошук кінетичних параметрів, з використанням методів пошукової оптимізації.

Результати. Отримані результати свідчать, що під впливом осмотичного, метаболічного стресу та гіпоксії уповільнюється робота аніонного обмінника AE1. Це відображується у зниженні константи швидкості обміну HCO_3^-/Cl^-, V_{max} обміну $H^+,SO_4^{2-}/Cl$. Прогнозоване зниження вмісту SO_4^{2-} іонів у клітинах підтверджують експериментальні дані. За результатами моделювання, інкубування клітин приводить до активації $Na^+,K^+,2Cl^-$-котранспортера і Na^+/H^+ обмінника і до гальмування потоку через $K^+,2Cl^-$-котранспортер. Оцінка складу мембранозв'язаного гемоглобіну свідчить, що зниження швидкості роботи AE1 обумовлено утворенням комплексу deoxyHb–B3p та окисними процесами у клітинах.

Висновки. Результати математичного моделювання й експериментальні дані свідчать про наявність універсальних O_2-залежних механізмів регулювання молекулярних процесів у еритроцитах, які базуються на конкуренції між deoxyHb та іншими білками за місця зв'язування з білком смуги 3.

Ключові слова: поглинання сульфату, транспорт аніонів, AE1, хлорид-бікарбонатний антипорт, аніонний обмін, мембранозв'язаний гемоглобін, лігандні форми гемоглобіну, геміхром, ферилгемоглобін

Received / Одержано	Revision / Доопрацьовано	Accepted / Прийнято	Published / Опубліковано
10 July, 2025	06 October, 2025	17 December, 2025	30 December, 2025